Fracture in mesoscopic disordered systems

Fracture in mesoscopic disordered systems

M. E. J. Karttunen*
Department of Electrical Engineering, Tampere University of Technology, P.O. Box 692, FIN-33101 Tampere, Finland and Research Institute for Theoretical Physics, P.O. Box 9, FIN-00014 University of Helsinki, Finland

K. J. Niskanen†
KCL Paper Science Centre, P.O. Box 70, FIN-02151 Espoo, Finland

K. Kaski‡
Department of Electrical Engineering, Tampere University of Technology, P. O. Box 692, FIN-33101 Tampere, Finland and Research Institute for Theoretical Physics, P.O. Box 9, FIN-00014 University of Helsinki, Finland
(Received 7 July 1993; revised manuscript received 29 November 1993)

A simple mechanical model of planar fibrous materials with mesoscopic disorder is introduced and analyzed. In this scalar model a shear modulus controls the stress transfer in the transverse direction. The system is studied using the effective medium approximation and computer simulations; the comparison between them is quite favorable. In the disorder-controlled regime the stress-strain relation, the number of broken cells at the onset of crack propagation, and the length of the final crack scale with the system size as L^2, $L^{1.7}$, and L, respectively. The mechanical properties are controlled by the interplay between disorder and shear modulus, which is studied in detail.

I. INTRODUCTION

Disorder plays a central role when mechanical properties of materials are considered. The subject of fracture behavior of disordered materials has been under extensive study especially during the last decade.[1–8] The interest is easily understandable on the basis of numerous applications from space technology to paper making. The effect of disorder depends on the properties under investigation. The strength and breakdown properties are highly dependent on disorder,[3,9] while elastic properties are not. The breakdown process itself enhances the effects of inhomogeneity.

Several models have been used in simulations of disordered materials. The most widely studied are the random fuse network,[2,3,5] elastic models such as the Born model[10,11] and different bond-bending[1,8] and beam models.[12] These studies have revealed many interesting properties, such as scaling[8,12] and multifractality;[12,13] even universality[8,13] has been proposed. However, the comparison of these models with experimentally studied systems is nontrivial and thus the practical counterparts of model parameters are ambiguous.[10] Nevertheless, phenomena such as gelation[1] and fracture of reservoir rocks[1,8] have been explained with the help of such simulation models.

Among disordered materials we focus our attention on planar fibrous materials, e.g., glass fiber networks, short fiber composites, and specifically ordinary paper. In a typical random fiber network there is disorder at two different length scales. At the microscopic length scale determined by the fiber length, disorder arises from the arrangement of fibers; their positions and orientations (sometimes also their lengths) are random. Thus a microscopic random fiber network corresponds to a lattice where the lattice constant and coordination number are random variables. On the other hand, at the mesoscopic length scale the local density varies and obeys Poisson distribution in the absence of spatial interfiber correlations.[14]

The microscopic structure of the fiber network shows up in the mesoscopic elastic and fracture properties. In a high-density network the fiber segments are short and transmit stresses far ahead of a propagating crack, while at low densities the network is flexible and tolerates large crack deformations without failing. Thus at the mesoscopic level the fracture behavior should depend on the elastic properties, particularly on the shear stiffness. At high shear stiffness disorder is irrelevant, while at low shear stiffness it dominates the fracture process. We study the interplay between elastic stress transfer and mesoscopic disorder using computer simulations and effective-medium approximation. Duxbury and Li[16] have already shown that a similar change in the fracture behavior can be affected by assigning residual strength to broken elements. In homogeneous materials the stress transfer mechanisms and residual strength affect the fracture toughness but do not change the nature of the fracture process (see, e.g., Ref. 15).

In order to confine the investigation to bare essentials, we have devised an elastic scalar model in terms of a lattice of adjoined (side-to-side) cells. These cells can be stretched in the longitudinal direction but they are not allowed to contract in the transverse direction. It is expected that, in any case, local variations in the contraction would not, if allowed, qualitatively change the fracture process. Our model resembles the random fuse network models[5,6] but its parameters are more closely related to those of real materials.

This paper is arranged as follows. In Sec. II we present the model. Then we describe the effective-medium theory

in Sec. III, followed by our results of finite-size scaling at strong disorder in Sec. IV. We present the results of the mechanical properties in Sec. V, and of the breaking characteristics and the related strength diagram. Section VI is dedicated to the discussion and conclusions.

II. THE MODEL

Our starting point is a microscopic random network consisting of fibers bonded to each other at interfiber crossings. The crossings divide the fibers into segments. If the bondings are stiff, the elastic energy of the network is given by the segment strains ε_i. For slender fibers or a low-density fiber network, the strains are predominantly axial, i.e., in the longitudinal x direction. The elastic energy of the network can be written as a sum over all the segments,

$$W=\frac{1}{2}\sum_i l_i\varepsilon_i^2 , \tag{1}$$

where l_i is the ith segment length and the fiber moduli are taken equal to unity. Despite its fibrous structure, the network can be considered continuous at a coarser mesoscopic level. It can be conveniently described by dividing it into a lattice of adjoined cells. The density of such a cell can be defined as

$$l_k=\sum_i l_i^k , \tag{2}$$

where the sum runs over all fiber segments in the kth cell and l_i^k is the part of the fiber segment i that is inside the kth cell. The random network structure implies that the cell density l_k has quenched disorder. We assume that l_k is uniformly distributed, $l_k\in[1-\rho,1+\rho]$. Thus the mean half-width ρ defines the density distribution. Similarly the cell strain is defined as the average strain of the fiber segments in cell k weighed by length:

$$\varepsilon_k=\frac{\sum_i \varepsilon_i l_i^k}{l_k} . \tag{3}$$

Because of the random orientation of the fibers, the strain ε_k is equal to one-half of the longitudinal (or areal) dilation of the cell.

As a first approximation it can be assumed that only the longitudinal degrees of freedom need to be considered, though the model can be readily generalized. In particular, different constitutive relations for the cells could be used. Therefore, we write the elastic energy of the lattice as

$$W=\frac{1}{2}\sum_k \alpha_k l_k\varepsilon_k^2+\frac{J}{8}\sum_{y-nn}(l_k+l_{ky})(\varepsilon_k-\varepsilon_{ky})^2 -\frac{h}{2}\sum_{x-nn}\varepsilon_k\alpha_{kx} . \tag{4}$$

The parameter α_k describes the damage of the kth cell: $\alpha_k=1$ for the cell that is intact and $\alpha_k=0$ for the broken cell. The cells are assumed linearly elastic up to a threshold strain ε_{th} at which they break completely and irreversibly ($\alpha_k=0$ if ε_k has ever exceeded ε_{th}).

The three energy terms in Eq. (4) are the self-energy of the cells, the coupling between transverse neighbors (ky) and the transmission of an external force h (Lagrange multiplier) to the longitudinal neighbors (kx). The first and third term describe the fact that—in the absence of transverse couplings—the stress along a longitudinal chain of cells should be constant. The stretching of a cell costs no energy if the cell is broken ($\alpha_k=0$), and no stress is transferred across the cell boundary from a broken longitudinal neighboring cell. The second term accounts for the fact that transverse neighbor pairs have a common boundary which—in the absence of longitudinal couplings—would prevent elongation differences between them. This would be the case even if the cells in question were broken, hence there is no α in the second term. It is clear that the model written in terms of local strains cannot describe global phenomena. For example, there is no penalty if adjacent longitudinal rows of cells are displaced by a constant amount relative to one another. However, the model captures, e.g., such essential features as stress concentration at crack tips and stress relaxation at crack boundaries. In addition, the cracks turn out to be straight lines which simplifies the scaling behavior of this model.

The only material parameter is the "shear modulus" J which is large at which densities of the underlying fiber network and small at low densities. Thus the model allows us to study how the flexibility of the fiber network affects the fracture behavior. This provides a direct link to real materials and to standard fracture mechanics.[15] A large J corresponds to a material with low fracture toughness and vice versa. Strength, on the other hand, goes up when J increases as will be shown below. The effect of J on the fracture process is easy to demonstrate by pulling apart, e.g., sheets of tissue paper (low density, hence small J) and tracing paper (high density, hence large J). We note that, as opposed to our cell model, in many of the ordinary lattice "bond" models[2,3,5] the stress transfer capacity cannot be varied independent of the Young's modulus. In many others[1,8,10–12] the model parameters have no counterparts in the properties of a continuum material, or the relationship between the model and a continuum material can be defined in several ways.

The local equilibrium is determined by $\partial W/\partial\varepsilon_k=0$. The equilibrium configuration for a given external force h is solved by using conjugate gradient method,[17] which is found to be computationally quite effective. Periodic boundary conditions are applied in the longitudinal and transverse directions. The adiabatic load-elongation behavior is determined in the usual manner.[4] First the cell that has the largest strain is broken (i.e., we set $\alpha_k=0$ for that cell). Then the new equilibrium strain configuration is calculated and the next chosen cell is erased. This process is continued until a crack crosses the sample. The stress-strain curve of the system is calculated from

$$\sigma_x=2\left[W+\frac{1}{2}h\sum_{x-nn}\varepsilon_k\alpha_{kx}\right]\Big/\varepsilon_x , \tag{5}$$

where the quantity in parenthesis is the internal energy and $\varepsilon_x = \langle \varepsilon_k \rangle$ is the macroscopic strain. For the numerical results we have taken averages over 1000 samples for the system size $L = 10$, 250 samples for $L = 20$–70, 100 samples for $L = 100$, and 20 samples for $L = 150$.

III. EFFECTIVE-MEDIUM APPROXIMATION

One expects intuitively that an effective-medium approximation (EMA) would be good as long as the local strain variations are small and no cells have failed.[18] This is the case in the elastic regime provided that the cell densities are uncorrelated and do not vary too much (ρ is small). A particular version of EMA may also work for the initial stages of fracture when only a small number of cells have failed.[19]

First we consider the elastic case, i.e., $\alpha_k \equiv 1$ for all k. The equilibrium configuration of cell strains is determined by $\partial W/\partial \varepsilon_k = 0$, or

$$\varepsilon_k = \frac{C}{l_k + J} \langle \varepsilon_k \rangle , \tag{6}$$

where ε_{ky} has been replaced with $\langle \varepsilon_k \rangle$ in the spirit of EMA. The proper value of $C = J + h \langle \varepsilon_k \rangle^{-1}$ depends on the distribution of cell densities $f(l_k)$ as the self-consistency condition $\int dl_k f(l_k) \varepsilon_k = \langle \varepsilon_k \rangle$ requires. Then a uniform distribution with $l_k \in [1-\rho, 1+\rho]$ yields

$$C = 2\rho / \ln[(1+\rho+J)/(1-\rho+J)] . \tag{7}$$

According to Eq. (6), the cells with the lowest density are strained most. The effect of cell density is strongest when the transverse coupling J is small. It is obvious that correlations between neighbor cells may cause substantial deviations from Eq. (6) and statistically significant simulation results would be difficult to obtain for comparison with EMA. On the other hand, for a uniform $f(l_k)$ the EMA distribution of cell strains $g(\varepsilon_k)$ is simple:

$$g(\varepsilon_k) = \text{const} \times \varepsilon_k^{-2} . \tag{8}$$

This result is found to agree with the simulation results irrespective of the values of J and ρ. Thus the intercell strain correlations are irrelevant. It is interesting that the EMA strain distribution in Eq. (8) is independent of J except for the normalization constant. Thus the geometric structure of the network, i.e., the spatial distribution of mass, totally determines the strain distribution.

Next we consider what happens when the first cell fails. This cell k must have the largest strain and according to Eq. (6) the smallest density, or $l_k = 1-\rho$. After the failure the strains of the broken cell k and its longitudinal and transverse neighbors are

$$\begin{aligned} \varepsilon_k &= [(C-J)/J]\varepsilon_x + \varepsilon_{ky} , \\ \varepsilon_{kx} &= [(C+J)/(2J+2)]\varepsilon_x , \\ \varepsilon_{ky} &= [(3C-2J)/(J+2)]\varepsilon_x . \end{aligned} \tag{9}$$

These values follow from the assumption that the strain deviates from the mean value $\varepsilon_x = \langle \varepsilon_k \rangle$ only in the broken cell and its immediate nearest neighbors.

It is easy to see from Eq. (9) that if ρ is small or J is large, then the strain ε_{ky} next to the first broken cell is larger than the strains in all the other unbroken cells. This happens when the following holds

$$\frac{3C-2J}{J+2} > \frac{C}{1-\rho+J} . \tag{10}$$

In this case the first failure triggers crack propagation across the system, a situation that might be called "single-crack" fracture. The (ρ, J) phase space for this behavior is shown in Fig. 1.

The extreme opposite to the case of single-crack fracture is that of strong disorder. In this case no crack propagation occurs.[5] Instead new failures appear at random locations, and a finite fraction of the cells have to be broken before the system fails. In considering the phase boundary between the strong disorder and the single-crack cases we assume that the cell failures affect only their immediate nearest neighbors but all other cells remain intact, i.e., $\varepsilon_k = \varepsilon_x$. In order to describe the situation let n_c be the critical number of broken cells in a crack that are needed before the crack becomes unstable (of course, at the same time many more cells have to be broken elsewhere in the system). The solid line in Fig. 1 corresponds to $n_c = 1$ and the dotted line to $n_c = 2$. When $J = 0$, the critical size n_c diverges as $n_c = 2\rho/(1-\rho)$, for $\rho \to 1$. Thus EMA predicts that the strong disorder behavior occurs only when $J \equiv 0$ and $\rho \equiv 1$.

The values for the stress and strain at which the first cell fails, σ_{init} and $\varepsilon_{\text{init}}$, respectively, are to a good approximation linear functions of the half-width ρ of the density distribution: $\sigma_{\text{init}} \sim \varepsilon_{\text{init}} \sim 1 - \text{const} \times \rho$. The positive constant depends on J and it is different for the two quantities, but becomes unity when $J \to 0$. On the other hand, the elastic modulus is a nonlinear function of ρ with a logarithmic singularity $E \sim -2/\ln(1-\rho)$, when $J = 0$ and $\rho \to 1$. For all these results the density distribution is assumed to be uniform.

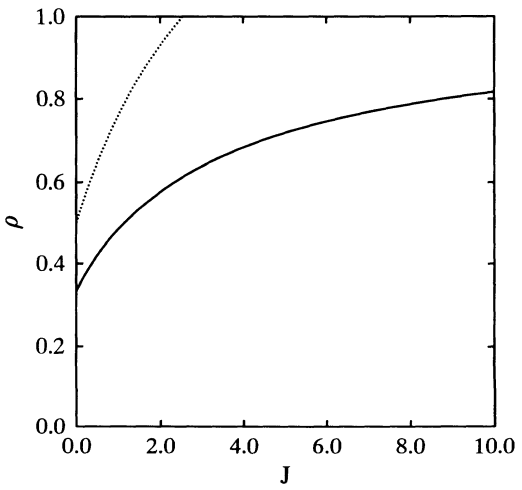

FIG. 1. EMA phase diagram, the first single crack is unstable below the solid line and the first twin crack below the dotted line.

IV. FINITE-SIZE SCALING AT STRONG DISORDER

The effective-medium approximation describes, by definition, infinitely large systems $L \to \infty$. Nevertheless, in analogy with several other studies[5,12] nontrivial finite-size effects are to be expected when disorder is sufficiently strong ($J \to 0$ or $\rho \to 1$). The fracture process can then be divided into three size-dependent regimes:[8] the initial fracture process dominated by the quenched disorder, the process of correlated but still nonlocalized failures, and the ultimate failure through crack propagation. The nature of the fracture process can be determined by monitoring certain characteristics for the first two phases. However, the description of the last phase is complicated by the fact that it is difficult to see, how much the propagation of the final, "fatal," crack is affected by cracks that already existed in the network. In our case the situation is simpler since the final crack always appears to go straight across the system.

One of the relevant quantities is the number of broken cells during the fracture process. The initial cracking at small external strain ε_x, should be random when the disorder is relevant.[12] Thus the external load F on the network should obey the following scaling relation as a function of the number of broken cells N:

$$F \sim L\Psi(N/L^2) . \tag{11}$$

This is indeed the case, since there is the data collapse to a single line for all N below some critical size-dependent value N_c as depicted in Fig. 2. Furthermore, Ψ is a linear function which follows directly from the fact that the residual stiffness and external strain of the system are both analytic functions of $N/L^2 \ll 1$.

The crack propagation begins at the point of the maximum stress $\sigma_{\max}=(F/L)_{\max}$, denoted by $N=N_{\max}(>N_c)$. This would correspond to the macroscopic rupture of a real sample. According to Herrmann, Hansen, and Roux,[12] $N_{\max}$ should scale as $N_{\max} \sim L^{1.75}$. Our simulation results (for $\rho=1, J=0.05$) are within error bars consistent with this showing an exponent 1.70 ± 0.06, as Fig. 3 illustrates. However, it is conceivable that the exponent could be larger in the limit $J \to 0$. In any case, the exponent value less than two shows that at the "thermodynamic" limit, $L \to \infty$, the fraction of broken cells at the onset of crack propagation vanishes when $\rho \equiv 1$ and $J > 0$. With increasing L and for smaller ρ values Fig. 3 also shows a crossover from this weak disorder behavior to the single-crack behavior. In the latter case the crack propagation starts from the first microcrack and thus $N_{\max} \to 1$ for $L \to \infty$.

Another quantity of interest is the total number of cells N_{tot} that have to be broken in order to break the sample into two parts. Because of the local nature of our scalar model, cracks are always straight transverse lines. Therefore, we expect N_{tot} to be given by

$$N_{\text{tot}} = N_{\max} + L - n_c , \tag{12}$$

where n_c is the critical crack size defined above (see Sec. III, i.e., n_c cells of the final crack are already counted for by $N_{\max}$). As Fig. 3 shows, Eq. (12) holds quite well, with $n_c > 2$ for $\rho = 1$. Again it can be seen that when $L \to \infty$, the single-crack behavior is obtained for $\rho < 1$. Thus $N_{\max} = n_c = 1$ and $N_{\text{tot}} \to L$ for $L \to \infty$.

The result given by Eq. (12) can be regarded as a special case of $N_{\text{tot}} = N_{\max} - n_c + N_{\text{crack}}$, where N_{crack} is the number of broken cells in the final macroscopic crack. This intuitively clear fact appears to have remained unappreciated. Since in our case the final crack appears *always* straight, the number of cells in it, N_{crack}, is larger than L only because some of the cracks created prior to the final crack happen to lie on its path. The number of them is in the first approximation equal to $2AL^{0.75}$,

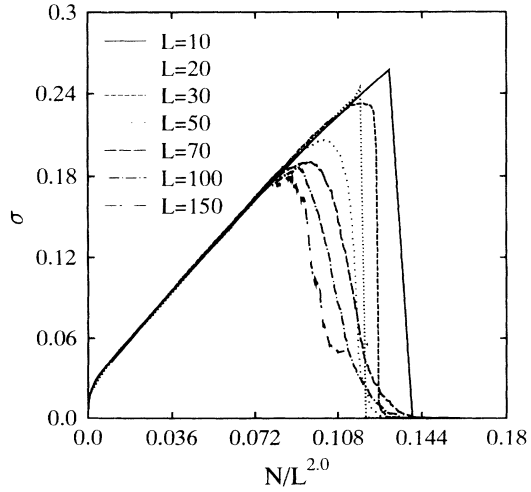

FIG. 2. Stress ($\sigma = F/L$) against the number of broken cells for $\rho = 1, J = 0.05$ at different system sizes.

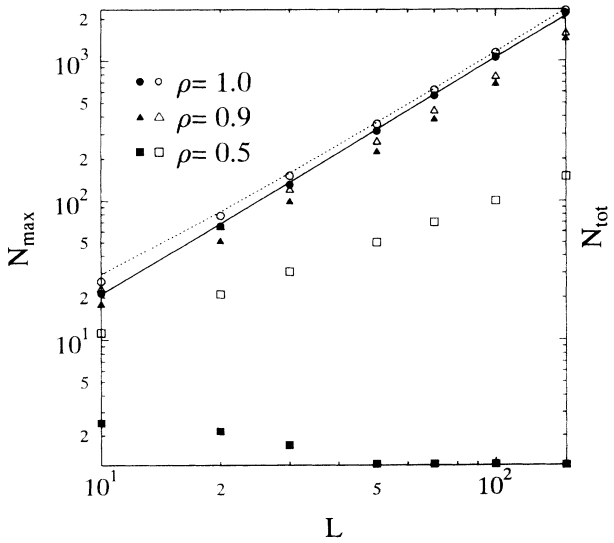

FIG. 3. Number of broken cells at the maximum stress ($N_{\max}$, filled symbols) and the total number of cell failures (N_{tot}, open symbols) as a function of system size for $J = 0.05$ and $\rho = 1.0$, 0.9, and 0.5 (bullets, triangles, and squares, respectively). Solid line corresponds to $N_{\max} \sim L^{1.7}$ and dotted line to Eq. (12) with $n_c = 2$.

where $A \approx 0.4$ is the scaling amplitude, given by $A = N_{\max} L^{-1.75}$. Therefore, in the limit of $L \to \infty$ we obtain $N_{\text{crack}} \approx L + 0.8 L^{0.75} \to L$. As a comparison, de Arcangelis and Herrmann found fractal cracks[2] to behave as $N_{\text{crack}} \sim L^{1.1}$. Much larger systems than what we have employed would be needed to confirm that N_{crack} in our case is indeed linear in the limit of $L \to \infty$.

When the load-elongation (stress-strain) behavior is considered, it is commonly assumed that the elastic modulus is independent of the system size. However, Sahimi and Arbabi[1] have recently argued that a very small logarithmic correction should be included:

$$F \sim \frac{L^{\Omega_1}}{(\ln L)^{\psi}} h(\lambda / L^{\Omega_1}) , \tag{13}$$

where $\Omega_1 \simeq 1.0 \pm 0.1$, $\psi \simeq 0.1$, and λ stands for elongation. The correction term follows from the analysis of the most critical defect by Duxbury, Leath, and Beale.[3] Also our simulations give some evidence for the existence of the logarithmic correction with exponent $\psi \simeq 0.1$. This exponent was found by monitoring the behavior of the standard deviation of the stress. However, in order to be conclusive about the logarithmic corrections to scaling, system sizes over several orders of magnitude should be studied.

V. MECHANICAL PROPERTIES

In addition to the size dependence, the mechanical properties of the disordered system are affected by the interplay between ρ and J. The shear coupling J tends to smooth out the density-induced strain variations. In other words, increasing J makes ρ effectively smaller. This is most clearly the case in the effective-medium approximation, where the cell strain is inversely proportional to $l_k + J$ [cf. Eq. (6)]. The combined effect of J and ρ is illustrated in Fig. 5. It can be seen that the simulated phase boundary from single crack to weak disorder fracture is consistent with the EMA result (Fig. 1).

From Fig. 4 it can be seen that the breaking stress, $\sigma_{\max}$, decreases slowly with increasing system size, as expected. When disorder is strong [Fig. 4(a)], the scaling part of the stress-strain curve is nonlinear, reflecting the fact that many cells have to be broken before the system fails. Then the breaking stress is strongly size dependent. Duxbury, Leath, and Beale[3] found for diluted random fuse network the asymptotic behavior $\sigma_{\max} \sim 1/\sqrt{\ln L}$. Our data seem to yield $\sigma_{\max} \sim 1/(\ln L)^{0.8}$ (Fig. 6) in agreement with Kahng *et al.*[5] In contrast, in the case of weak disorder [Fig. 4(b)] the first failure determines the system strength when $L \to \infty$. In that case, the breaking stress depends on the system size only when the size is small (cf. Fig. 6). In other words, if the density distribution (and hence the strain distribution) is narrow, a small system suffices to sample its strength.

The effect of ρ and J on the breaking stress is shown in Fig. 7(a). The linear decay of $\sigma_{\max}$ with increasing ρ corresponds to single-crack fracture and agrees with the result obtained from the effective-medium approximation (cf. Sec. III and observe that in this case $\sigma_{\max} = \sigma_{\text{init}}$).

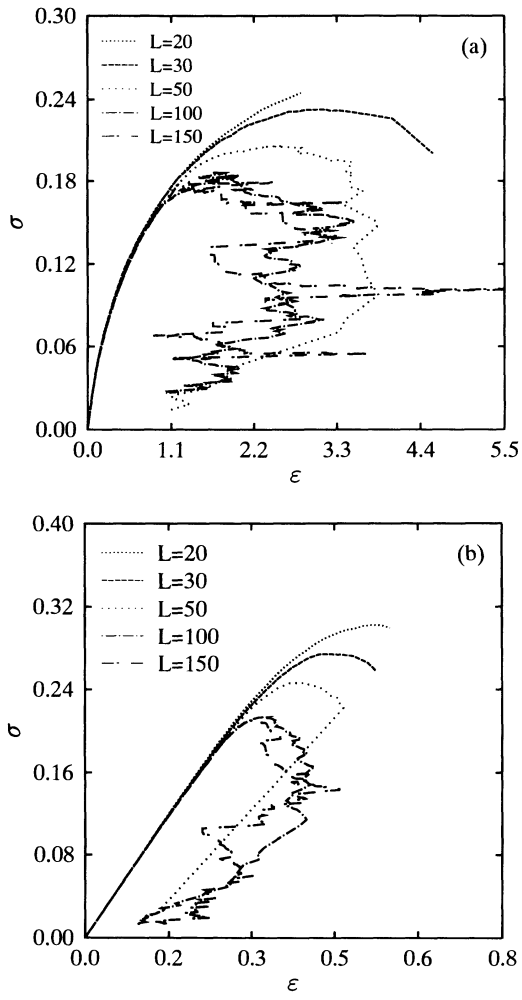

FIG. 4. Stress-strain curves at different system sizes for (a) $\rho = 1.0$, $J = 0.05$ and for (b) $\rho = 1.0$, $J = 1.0$.

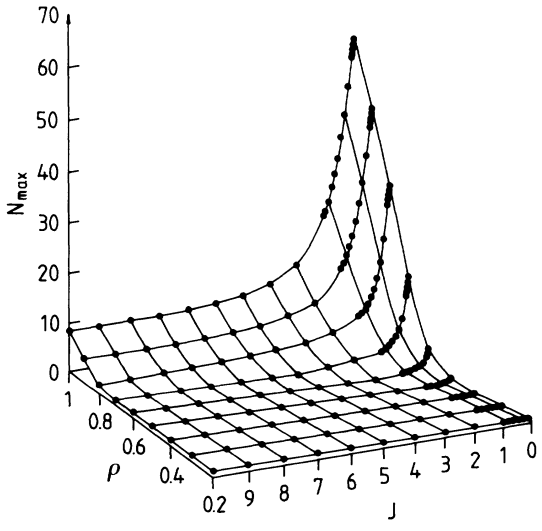

FIG. 5. Number of broken cells at the maximum stress ($N_{\max}$) as a function of J and ρ for system size $L = 20$.

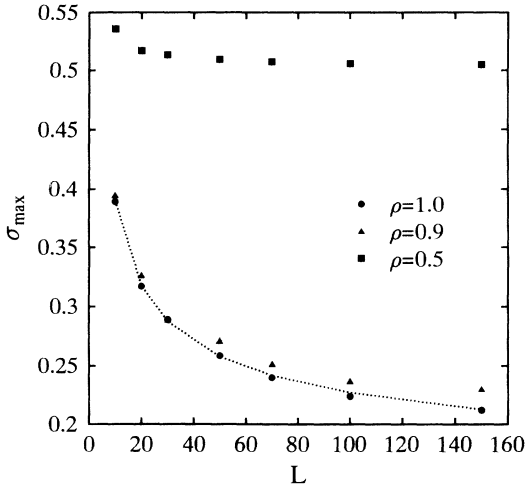

FIG. 6. Breaking stress (σ_{max}) as a function of system size L for $J=0.05$ and $\rho=1.0$, 0.9, and 0.5 (bullets, triangles, and squares, respectively). Dotted line corresponds to $\sigma_{max} \sim 1/(\ln L)^{0.8}$.

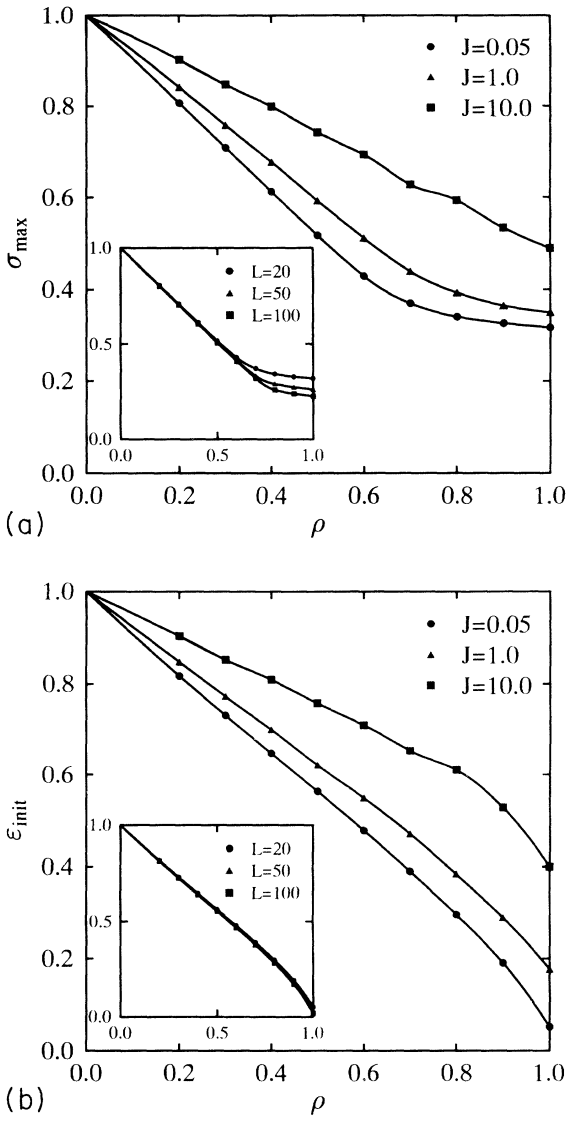

FIG. 7. (a) Breaking stress (σ_{max}) and (b) the strain at which the first cell fails (ε_{init}) as a function of ρ for $J=0.05$, 1.0, and 10.0 (bullets, triangles, and squares, respectively) at $L=20$. The insets show the result at $J=0.05$ for system sizes $L=20$, 50, and 100.

The plateau at large ρ and small J corresponds to weak disorder behavior. As the inset in Fig. 7(a) shows, the transition from single crack to weak disorder occurs for ever larger ρ when the system size grows. Also, the *strain* values pertinent to the fracture process follow closely the linear trend implied by EMA, except in the limit of $\rho \to 1$ [Fig. 7(b)]. When $\rho \equiv 1$ weak disorder behavior is obtained for all J and hence σ_{max} and ε_{init} are size dependent. If J is small the stress-strain curve is nonlinear [Fig. 4(a)] and thus $\varepsilon_{init} < \sigma_{max}$ even though the elastic modulus of the system is always less than or equal to unity. On the other hand, when J grows, the stress-strain curve becomes linear [Fig. 4(b)].

VI. DISCUSSION

In this paper, we have reported results for a scalar model with disorder at mesoscopic length scale at which the materials of interest—such as disordered fiber networks—can be considered continuous. Hence the elastic energy of the system is defined using as independent variables the strains of lattice cells instead of the strains of, e.g., lattice bonds. The approach proves quite useful and illustrative. Furthermore, this approach is solvable with the effective-medium approximation, which in turn is capable of explaining a good deal of the behavior of the model.

Depending on its parameters the model exhibits single-crack and weak disorder fracture. In addition, strong disorder fracture is suggested by the nontrivial finite-size scaling, $N_{max} \sim L^{1.7}$ but only when $(\rho \to 1)$, $(J \to 0)$, *and* $(L \to \infty)$. Because of the straight cracks the model yields, the total number of cell failures is given by Eq. (12). This is a special case of $N_{tot} = N_{max} - n_c + N_{crack}$, where N_{crack} is the number of broken cells in the final macroscopic crack. The intuitively clear relationship explains the crossover in the finite-size scaling of N_{tot} from the single-crack to the strong disorder behavior. In our case $N_{crack}/L \to 1$ when $L \to \infty$ even in the case of strong disorder.

Our model illustrates also how sufficiently large elastic systems always fail through a single crack except for sufficiently strong disorder $\rho \to 1$. The precise location of the phase boundary between single crack and weak disorder fracture remains unclear in the present case but a reasonable estimate for $L \to \infty$ is obtained from the effective-medium approximation. Experimentally the crossover in the fracture mode can be demonstrated with, e.g., paper samples. Small samples fail gradually with a "post-fracture tail" in the stress-strain curve whereas

large samples tear apart.[20] The same crossover can also be effected by increasing the shear coupling (relative to Young's modulus) as given by J in the model: A strong coupling leads to high stress concentrations at the crack tip and thus favors crack propagation. In real paper this happens, e.g., when the average mass per unit area is increased.[21]

It should be noted that even in the case of weak disorder a dominant crack emerges eventually and its growth controls the ultimate failure. The stability of crack growth can be analyzed using the standard concepts of fracture mechanics such as fracture toughness.[15] Disorder is generally irrelevant in such considerations. On the other hand, the onset of the macroscopic failure process or crack propagation is controlled by different factors and then the role of disorder is important. For example, the above results show that if disorder is *irrelevant* (i.e., the first crack is unstable), the breaking stress decreases with increasing disorder: $\sigma_{\max} \sim 1 - \text{const} \times \rho$. On the other hand, if disorder is large enough, and thus relevant, then $\sigma_{\max}$ is *independent* of ρ. This perhaps surprising situation has apparently not been realized before when the strength of disordered materials such as paper has been analyzed. Rather than studying what happens as a function of disorder—which is often difficult to control—it appears better to consider the size dependence of the breaking characteristics.

This investigation has been motivated by the desire to model the behavior of continuous disordered materials, especially fiber networks with mesoscopic disorder. In that respect several questions remain open. For example, what are the physical dimensions of the lattice cells? Disorder becomes weaker if cells are made larger but they fail more gradually which enhances the effect of disorder.[16] Another issue of interest is the effect of the plastic deformations that occur in real materials. Work is in progress to address these questions.

ACKNOWLEDGMENTS

The simulations were done using Stardent Titan 3000 and the DEC 3000-500 AXP computers of Electronics Laboratory and Computing Center of Tampere University of Technology. This study was partially supported by Suomen Luonnonvarain Tutkimussäätiö and by the Technology Development Centre of Finland. The authors also wish to thank Professor P. Leath for critical reading of this paper and comments.

*Present address: Department of Physics, Rutherford Building, McGill University, 3600 rue University, Montréal (Qué.), Canada H3A 2T8.

†Address until 1 July 1994: USDA Forest Service, Forest Products Laboratory, One Gifford Pinchot Dr., Madison, WI 53705-2398.

‡Present address: Theoretical Physics, Department of Physics, University of Oxford, 1 Keble Road, Oxford OX1 3NP, United Kingdom.

[1]S. Arbabi and M. Sahimi, Phys. Rev. B **47**, 695 (1993); M. Sahimi and S. Arbabi, *ibid.* **47**, 703 (1993).

[2]L. de Arcangelis and H. J. Herrmann, Phys. Rev. B **39**, 2678 (1989).

[3]P. M. Duxbury, P. L. Leath, and P. D. Beale, Phys. Rev. Lett. **57**, 1052 (1986); Phys. Rev. B **36**, 1 (1987).

[4]H. J. Herrmann and S. Roux, in *Statistical Models for The Fracture of Disordered Media,* edited by H. J. Herrmann and S. Roux (Elsevier Science, Amsterdam, 1990), Chap. 5.

[5]B. Kahng, G. G. Batrouni, S. Redner, L. de Arcangelis, and H. J. Herrmann, Phys. Rev. B **37**, 13 (1988).

[6]L. de Arcangelis, S. Redner, and H. J. Herrmann, J. Phys. (Paris) Lett. **46**, L585 (1985).

[7]P. Meakin, G. Li, L. M. Sander, E. Louis, and F. Guinea, J. Phys. A **22**, 1393 (1989).

[8]M. Sahimi and S. Arbabi, Phys. Rev. B **47**, 713 (1993).

[9]P. M. Duxbury, P. D. Beale, and P. L. Leath, Phys. Rev. Lett. **57**, 1052 (1986).

[10]S. Feng and P. N. Sen, Phys. Rev. Lett. **52**, 216 (1984).

[11]M. J. Alava and R. K. Ritala, J. Phys.: Condens. Matter **2**, 6093 (1990).

[12]H. J. Herrmann, A. Hansen, and S. Roux, Phys. Rev. B **39**, 637 (1989).

[13]A. Hansen, E. Hinrichsen, and S. Roux, Phys. Rev. B **43**, 665 (1991).

[14]H. Corte and O. J. Kallmes, in *Formation and Structure of Paper,* edited by F. Bolam (British Paper and Board Makers Association, London, 1962), p. 13; see also C. T. J. Dodson, J. Pulp Paper Sci. **18**, J74 (1992), and references therein.

[15]M. F. Kanninen and C. H. Popelar, *Advanced Fracture Mechanics* (Oxford University Press, New York, 1985).

[16]Y. S. Li and P. M. Duxbury, Phys. Rev. B **38**, 9257 (1988).

[17]M. Hestenes, *Conjugate Direction Methods in Optimization* (Springer-Verlag, Berlin, 1980).

[18]See, e.g., H. J. Herrmann and S. Roux, in Ref. 4, Chap. 5.

[19]A. Hansen, S. Roux, and H. J. Herrmann, J. Phys. Paris **50**, 733 (1989).

[20]J. Goldschmidt and D. Wahren, Sv. Papperstidn. **71**, 477 (1968).

[21]H. Corte, Das Papier **16**, 575 (1962).